International Journal of Nanomedicine

Dovepress
open access to scientific and medical research

Open Access Full Text Article

ORIGINAL RESEARCH

Carbon nanotubes impregnated with subventricular zone neural progenitor cells promotes recovery from stroke

This article was published in the following Dove Press journal:
International Journal of Nanomedicine
31 May 2012
Number of times this article has been viewed

Sung Ung Moon[1,*]
Jihee Kim[1,2,*]
Kiran Kumar Bokara[1,*]
Jong Youl Kim[1]
Dongwoo Khang[3,4]
Thomas J Webster[3,4]
Jong Eun Lee[1,2]

[1]Department of Anatomy, [2]Brain Korea 21 Project for Medical Science, Yonsei University College of Medicine, Seoul, South Korea; [3]School of Engineering, [4]Department of Orthopedics, Brown University, Providence, RI, USA

*These authors contributed equally to this work

Abstract: The present in vivo study was conducted to evaluate whether hydrophilic (HL) or hydrophobic (HP) carbon nanotubes (CNTs) impregnated with subventricular zone neural progenitor cells (SVZ NPCs) could repair damaged neural tissue following stroke. For this purpose, stroke damaged rats were transplanted with HL CNT-SVZ NPCs, HP CNT-SVZ NPCs, or SVZ NPCs alone for 1, 3, 5, and 8 weeks. Results showed that the HP CNT-SVZ NPC transplants improved rat behavior and reduced infarct cyst volume and infarct cyst area compared with the experimental control and the HL CNT-SVZ NPC and SVZ NPCs alone groups. The transplantation groups showed an increase in the expression of nestin (cell stemness marker) and proliferation which was evident with the increased number of doublecortin and bromodeoxyuridine double-stained immunopositive cells around the lesion site. But, these effects were more prominent in the HP CNT-SVZ NPC group compared with the other transplantation groups. The HP CNT-SVZ NPC and HL CNT-SVZ NPC transplants increased the number of microtubule-associated protein 2 (marker for neurons) and decreased the number of glial fibrillary acidic protein (marker for astroglial cells) positive cells within the injury epicenter. The majority of the transplanted HP CNT-SVZ NPCs collectively broadened around the ischemic injured region and the SVZ NPCs differentiated into mature neurons, attained the synapse morphology (TUJ1, synaptophysin), and decreased microglial activation (CD11b/c [OX-42]). For these reasons, this study provided the first evidence that CNTs can improve stem cell differentiation to heal stroke damage and, thus, deserve further attention.

Keywords: biocompatibility, brain, in vivo, stem cell, wettability, carbon nanotubes, stroke

Introduction

In recent years, the design of biomaterials has evolved from the classical, first generation material-based approach that favored mechanical strength, durability, bioinertness, and biocompatibility to one that seeks to incorporate instructive signals into scaffolds to modulate cellular functions such as proliferation, differentiation, and morphogenesis.[1] To impart bioactivity to these biomaterials, their surfaces may be adorned with signaling molecules such as glycosaminoglycans, proteoglycans, and glycoproteins normally associated with the extracellular matrix (ECM) on cell surfaces, or they may be loaded with soluble bioactive molecules such as chemokines, cytokines, growth factors, or hormones which could enhance paracrine effects.[1] In the central nervous system (CNS), neural cells adhere to the fibrillar protein meshwork known as the ECM. Dynamic cell ECM interactions trigger specific cell signaling and maintain proper cell growth, differentiation, and survival. A loss of cell–ECM contacts may cause cell apoptosis.[2,3] In the ECM, there is a microenvironment (niche),

Correspondence: Jong Eun Lee
Department of Anatomy, Brain Korea 21 Project for Medical Science, Yonsei University College of Medicine, 250 Seongsanno, Seodaemun-gu, Seoul 120-752, South Korea
Tel +82 2 2228 1646
Fax +82 2 365 0700
Email jelee@yuhs.ac

Thomas J Webster
184 Hope Street, School of Engineering, Brown University, Providence, RI 02912, USA
Tel +1 401 863 2318
Fax +1 401 863 1309
Email thomas_webster@brown.edu

in which extrinsic signals such as ECM proteins and soluble factors from other cells control progenitor cell proliferation and fate.[2,3] It is for this reason that nanotechnology (or the use of nanostructured materials that mimic the biological milieu) has attracted so much attention in biomaterials. Only nanoscale biomaterials mimic the natural structure and topography of the ECM.

Many researchers have indeed used nanostructured biomaterials to stimulate mature cell types such as epithelial cells, fibroblasts, muscle cells, and neurons.[4,5] This nanosensitivity has recently been extended to the differentiation of various stem cells including mesenchymal stem cells.[6] More importantly, the influence of surface features or topography on differentiated cellular growth, movement, and orientation has long been recognized.[7–10] For example, adult hippocampal progenitor cells, cocultured with postnatal rat type-1 astrocytes, were found to be extended axially along the grooves of micropatterned polystyrene substrates which were chemically modified with laminin.[11] Directionally aligned poly(L-lactide) nanofibrous scaffolds fabricated by electrospinning induce neural stem cells (NSCs) to align themselves parallel to the fibers.[12] Microcontact printing of neuron-adhesive peptides using polydimethylsiloxane soft lithography has provided a valuable tool for studying axonal guidance and neurite formation in developmental neurobiology.[13] Substrate nanopatterning holds particular utility in neural tissue engineering because repair of neurological injuries often requires directional guidance in terms of neuronal growth, migration, neurite projection, or synapse formation.[2,14] In addition, McBeath et al demonstrated that the fate of mesenchymal stem cell differentiation can be altered by manipulating cell shape using a micropatterned adhesive substrate.[15]

Lastly, the effect of surface wettability on cell–biomaterial interactions has been extensively studied. Its importance in the design of implantable scaffolds was first reported by Weiss in 1960,[16] later confirmed by many others.[5,17–22] Since cells effectively adhered onto polymer surfaces with moderate wettability as demonstrated by water contact angles of 40–70 degress,[23–27] it is clear that the wettability of a biomaterial surface plays a critical role in cell attachment and proliferation.[28–30] In addition, it has been shown that most human bone marrow stromal cells attached to hydrophobic (HP) surfaces had smaller surface contact areas, resulting in a more rounded cell morphology.[28]

Of course, the CNS has limited regenerative potential when inflicted with lesions resulting from trauma, stroke, or neuropathological conditions. Repair from neurological injuries in the CNS is complicated by the presence of inhibitors for nerve regeneration, notably neurite outgrowth inhibitors and myelin-associated glycoproteins.[31] Recently, stem cell research has provided hope for replacing lost neuronal cells for several neurodegenerative diseases. Functional recovery following brain and spinal cord injuries likely require the transplantation of exogenous NSCs and tissues, since the mammalian CNS has little capacity for self-repair.[1,32,33] Also, clinical trials using the transplantation of NSCs to treat neurodegenerative diseases such as stroke has raised questions regarding the effectiveness of this strategy.[34]

NSCs are defined as self-renewing, primordial cells with the capacity to give rise to a differentiated progeny with all neural lineages, and are posited to exist in embryonic and fetal germinal zones where they participate in CNS organogenesis.[35,36] In the adult mammalian brain, NSCs were reported from two specific regions, the subventricular zone (SVZ) and the dentate gyrus area of the hippocampus,[37] and it remains to be determined whether these NSCs also participate in self-repair mechanisms. It is known that cells with stem cell-like characteristics can be isolated from the mammalian CNS at all ages, propagated in culture, and reimplanted into injured CNS regions.[31,36,38–41] However, previous studies suggested that endogenous self-repair capacity is not enough to compensate for damaged neural tissues,[1,32,33] and the transplantation of exogenous neural cells or tissues have limitations because of low survival rate at the injury sites.[33] Approaches towards enhancing the survival rate of the transplanted NSCs include an alternative strategy for building biological substitutes, such as a three-dimensional culture of neural cells to repair or replace the function of damaged nerve tissues. Tissue engineering in combination with neural cells may generate functional three-dimensional constructs to serve as a replacement for damaged tissues or organs.[2,42,43] Among the various biomaterials available, carbon nanotubes (CNTs) are one of the most attractive candidates for therapeutic strategies.

Of late, among many types of biomaterials available, CNTs have attracted much attention in the neural biomaterials' field since they have been shown to be electrically active,[44] can be formulated to match the dimensions of components of brain tissue such as laminin,[45–49] and their wettability can be easily controlled. Previous in vitro studies have measured increased neurite and axonal outgrowth from neurons on carbon nanofibers/CNTs compared to currently used nervous system implants such as silicon.[48] It was also reported that CNT substrates, which boost neuronal electrical signaling,[44]

decrease astrocyte formation and macrophage density (cells which synthesize unwanted glial scar tissue in the brain when overstimulated) compared to silicone implants in vitro.[48] Other in vitro studies have examined the potential use of carbon nanofibers/CNTs in orthopedic applications triggering in vitro bone formation and decreasing fibrous scar tissue formation compared to conventional materials used in orthopedics such as titanium.[49]

Previously, it was reported that CNTs can increase the differentiation of NSCs to neurons[50] and CNTs can decrease macrophage activation, which collectively indicates promise for the use of CNTs as novel stem cell delivery vehicles for treating stroke damaged neural tissue.[51,52] These attractive properties of CNTs have been attributed to their unique conductivity and surface energetics capable of promoting the adsorption of endogenous proteins important for mediating cell adhesion (particularly the adsorption of vitronectin and fibronectin).[53–55] CNTs have been exploited due to their "cell-friendly" nature which aids in promoting the functions of damaged neurons.[48] Specifically, researchers have developed micron patterns of CNTs on polymers such as polycarbonate urethane, which enable neuron cell attachment and extension of neurites along CNT regions. These results highlight the ability of CNTs to direct functions of neurons to potentially heal damaged neural tissue.[48,50]

The current study continues such promising work to determine in vivo if CNTs impregnated with SVZ neural progenitor cells (NPCs) could treat rats with stroke-induced brain damage 1, 3, 5, or 8 weeks postinjury. Promising results suggest that CNTs should be studied further to return motor function to stroke induced patients.

Material and methods

Substrates

CNTs were purchased from Applied Sciences, Inc (Cedarville, OH). They possessed diameters of either 60 nm or 100 nm and lengths of up to 5 μm. The surface energy of the CNTs was controlled by the presence or absence of a hydrocarbon outer layer.[47,49] CNTs with a hydrocarbon outer layer (100 nm diameters in which the hydrocarbon outer layer was formed naturally during the carbon vapor deposition synthesis) possessed relatively HP surface properties (HP CNTs) compared to those without the hydrocarbon outer layer (60 nm diameter, termed hydrophilic [HL CNTs] here).[47,49] Specifically, as previously determined, the surface energy of the HL CNTs and HP CNTs were 120–140 mJ/m^2 and 75–95 mJ/m^2, respectively.[47,49]

SVZ NPCs and bromodeoxyuridine (BrdU) labeling

NPCs from the SVZ of mice were obtained through well-established procedures. Briefly, the brains of 1–3 day old neonatal mice were removed from the skull and fragments of the SVZ (500 μm-thick coronal sections encompassing both ependymal and subependymal layers) were dissected and placed in Hank's buffered saline solution (Invitrogen, Grand Island, NY). The brains were then digested in a Gibco® solution containing 0.025% trypsin and 0.25 mM ethylenediaminetetraacetic acid (Invitrogen Life Technologies, Carlsbad, CA) and triturated to collect the SVZ NPCs. Resulting SVZ NPCs were then plated in six-well plates at a density of 5.0×10^5 cells/mL. Upon attaining confluency, NPCs were then collected from cell culture plates and injected immediately at the same density, time, and volumes into rat brains as described below. One hour before injection, 10 μM of BrdU (Sigma-Aldrich Corporation, St Louis, MO) was applied to synchronized cell cultures for BrdU prelabeling.

In vivo model

Animals

For this study, male Sprague–Dawley rats from Samtako (Osan, South Korea) were used. All animal procedures were conducted according to a protocol approved by the Yonsei University (Seoul, South Korea) Animal Care and Use Committee in accordance with National Institutes of Health guidelines. Male Sprague Dawley rats (Osan, South Korea) weighing 300–330 g were used. Rats were kept on a 12-hour light/dark cycle with ad libitum access to food and water. Rats were acclimated for 3 days before experimentation.

Focal cerebral ischemia model

Male rats (300–330 g) were subjected to 90 minutes of transient middle cerebral artery occlusion (MCAO, n = 50). Animals were anesthetized with a ketamine cocktail (300 mg/kg) intramuscularly. The depth of anesthesia was assessed by a toe pinch at every 15 minutes. Rectal temperature, respiration, and heart rate were monitored and maintained in the physiological range throughout the surgery. Focal cerebral ischemia was induced using an occluding intraluminal suture.[56,57] Briefly, the rat was placed on a stereotaxic frame 5002 (David Kopf Instruments, Tujunga, CA). A craniectomy (3 mm in diameter, 6 mm lateral and 2 mm caudal to the bregma) was performed with extreme care over the MCA territory using a trephine (RTX-1-KR, Black & Decker, Korea). The dura mater was left intact and a laser Doppler flowmeter probe was placed on the surface of the ipsilateral cortex and fixed to the periosteum. The probe

was connected to a laser flowmeter device (Omegaflo FLO-C1; Omegawave Inc, Tokyo, Japan) for continuous monitoring of regional cerebral blood flow. The left carotid artery and its branches were exposed through a midline cervical incision. The left external carotid artery was tied by a 3 mm monofilament nylon to block its branches. In brief, an uncoated 30 mm segment of a 3 mm Dermalon™ suture (blue monofilament nylon DG; Ethicon Inc, Somerville, NJ) with the tip rounded by a flame was inserted into the arteriotomy and advanced under direct visualization into the internal carotid artery 20–25 mm from the bifurcation to occlude the ostium of the MCA, until regional cerebral blood flow was reduced to 15%–20% of the baseline (recorded by a laser Doppler flowmeter). After 90 minutes of occlusion, the suture was pulled back to restore the blood flow (confirmed by the return of regional cerebral blood flow to the baseline level), the site on the arteriotomy was tied and surgical incisions were closed. Animals were allowed to recover. Twenty-two hours later, the animals were euthanized with an isoflurane overdose. The brains were removed and 2-mm thick blocks were cut in the coronal plane, stained with 2% triphenyl tetrazolium chloride (TTC; Sigma-Aldrich) to delineate regions of infarction, and embedded in paraffin. After paraffin embedding, 5-µm thick sections were stained with hematoxylin and eosin (Mutopure Chemicals Co. Ltd, Tokyo, Japan). The initial stroke damage was confirmed via magnetic resonance imaging (3.0 Tesla MR system, Intera Achieva, Philips Medical Systems, Netherlands) and TTC staining.

A 2–3 mm hole was drilled over the skull and the probe was placed over the brain in a region corresponding to the ischemic core. Stable readings were obtained before advancing the suture, and regional cerebral blood flow was determined using laser Doppler flowmetry and expressed as the percentage change from baseline. Regional cerebral blood flow was estimated at four different times: before and during MCAO (90 minutes), and 1 hour and 2 hours after reperfusion in all the experimental groups.[56,57]

Ischemic lesion analysis and microinjection of CNTs impregnated with SVZ NPCs

An initial image of the brain lesion was obtained using in vivo magnetic resonance imaging (Figure 1B-b). Also, rats

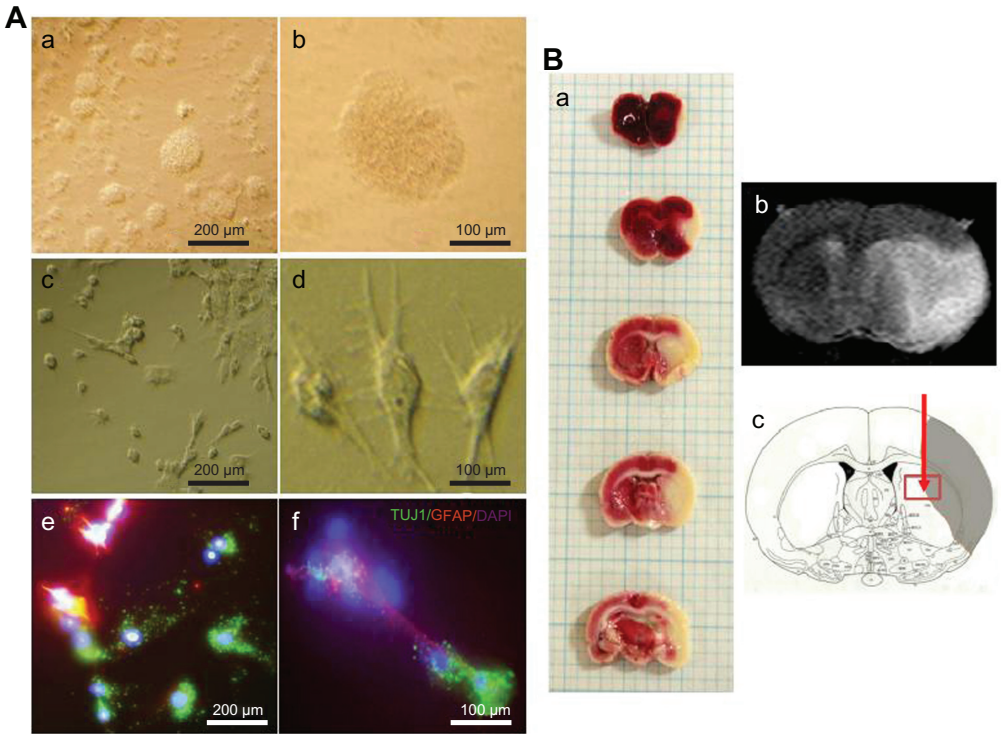

Figure 1 (**A**) Phase contrast images of subventricular zone neural progenitor cells and their cell lineage in vitro. The subventricular zone neural progenitor cells grown in the culture media have a neurosphere form (a and b). After two weeks of culture, the subventricular zone neural progenitor cells were differentiated primarily into neurons (60%–70%) and glial cells (c and d), which were detected by staining them with a neuronal marker (TUJ1) and an astrocyte marker (glial fibrillary acidic protein) (e and f). The nucleus of the cells was counterstained with 4′,6-diamidino-2-phenylindole. Scale bars = 100 µm and 200 µm. (**B**) The determination of ischemic lesion and transplantation of subventricular zone neural progenitor cells in the ischemic injured brain in vivo. The infarct area after middle cerebral artery occlusion injury was verified by triphenyl tetrazolium chloride staining (a) and magnetic resonance imaging (b). The subventricular zone neural progenitor cells impregnated with carbon nanotubes were transplanted into the injured brain directly by microinjection (c).

Abbreviations: DAPI, 4′,6-diamidino-2-phenylindole; GFAP, glial fibrillary acidic protein.

were sacrificed at 24 hours postsurgery and TTC staining was completed to demonstrate the infarct in real size, which was characterized with structural disintegration (Figure 1B-a). A vibrissae reflex test was also completed to confirm brain injury 24 hours after MCAO. After confirmation of neural damage, rats were anesthetized with a ketamine cocktail (300 mg/kg) and then positioned on a stereotaxic apparatus (David Kopf). Microinjection (0.2 mm posterior from the bregma, 2 mm lateral from the sagittal suture, and 4.5 mm below the dura mater) of SVZ NPCs (5.0×10^5 cells/10 μL) and each type of CNTs impregnated with SVZ NPCs (ie, HP CNT-SVZ NPC and HL CNT-SVZ NPC transplants) was completed using a 31 gauge needle through a dentist's burr hole onto the upper striatum of the rat brains which possessed stroke damage. Then, the rats were sacrificed after 1, 3, 5, and 8 weeks from transplantation.

Infarct volume assessment

Animals were deeply anesthetized with chloral hydrate (Sigma-Aldrich) at 1, 3, 5, and 8 weeks postinjury in the SVZ NPCs alone or CNTs impregnated with SVZ NPC transplantation groups. The experimental groups were transcardially perfused with heparinized saline followed by 4% paraformaldehyde. The brains were postfixed with 4% paraformaldehyde 16–24 hours. Later, the brains were sliced into coronal sections 2 mm thick using a rat brain matrix (Ted Pella, Redding, CA). The sliced brain tissues were embedded in paraffin, and then were sectioned into 4 μM thickness using a microtome and were stained by hematoxylin and eosin. The volume of cerebral tissue infarction was determined from hematoxylin and eosin-stained sections (12 sections per animal). Using OPTIMUS® 6.0 software (OPTIMUS Corporation, Fort Collins, CO), the area of the infarct cyst of both hemispheres were measured by tracing them on the computer screen. Infarct volume (mm^3) was calculated by averaging the area of injury recorded from each slide. The value was multiplied by the total distance between the first and last sections (ie, from the beginning of infarct cyst until the end of the cyst).[58]

Histological examination

Rats were anesthetized with chloral hydrate and decapitated 22 hours after MCAO. Rat brains were cut into coronal slices 2 mm thick using a rat brain matrix (Ted Pella). The brain slices were fixed with 4% paraformaldehyde (pH 7.4) in 0.1M phosphate buffered saline (Sigma-Aldrich) for 1 day and subsequently embedded in a paraffin block. After paraffin embedding, 5 μm thick sections were used either for hematoxylin and eosin staining or for immunostaining.[59]

Immunohistochemistry

After the end of the prescribed time periods, healing of the damaged brain tissue was measured from histological sections and injected SVZ NPCs were immunostained with an anti-BrdU antibody (Lab Vision, Fremont, CA) before transplantation. The injected SVZ NPCs were typified by immunostaining with nestin (a marker for NPCs; Millipore Biosciences Research Reagents, Temecula, CA), microtubule-like associated protein 2 (MAP2, a marker for fully differentiated neurons; Sigma-Aldrich), TUJ1 (a marker for early neurons and mature neurons; Covance Inc, Berkeley, CA), glial fibrillary acidic protein (GFAP, a marker for astrocytes; Millipore), and CD11b/c (OX-42, a marker for reactive microglial cells; Abcam, Cambridge, MA), followed by an appropriate biotinylated secondary antibody. Staining was visualized using the Zymed® Histostain-Plus Bulk kit (Invitrogen) and then reacted with diaminobenzidine (Sigma-Aldrich) or Fast-Red (Lab Vision). The secondary antibodies for immunofluorescence staining were goat antirabbit immunoglobulin G fluorescein isothiocyanate (Millipore) and goat anti-mouse immunoglobulin G rhodamine (Millipore). Immunostaining controls were prepared by incubating cells or tissues without primary antibodies. All incubation steps were performed in a humidified chamber. In this manner, increased staining of nestin and TUJ1 would indicate NPC differentiation into neurons while increased staining for GFAP would indicate glial scar tissue formation. To confirm a neurocircuit and synapse formation around CNTs, synaptophysin (Sigma-Aldrich) and TUJ1 antibodies were used. Furthermore, doublecortin (DCX; Abcam) was used to indicate migrating NPCs and OX-42 positive cells and to indicate reactive microglia cells around CNTs, the injury area, and scar regions. The SVZ NPCs were counterstained with 4′6-diamino-2-phenylindole (DAPI) for 10 min at room temperature for nuclear visualization. Controls consisted of the transplantation of SVZ NPCs without CNTs, and negative controls for experimental groups were the MCAO-subjected animals without SVZ NPC transplantation.

Neurological functional tests

Rotarod test

An accelerating rat rotarod (47700; Ugo Basile, Comerio, Italy) was used to measure rat motor function and balance. The rats were placed on the rotarod cylinder and the time the animals remained on the rotarod was recorded. The speed was slowly increased from 4 rpm to 40 rpm within 5 minutes. A trial ended if the animal fell off from the rungs or gripped the device and spun around for two consecutive revolutions without attempting to walk on the rungs. The animals were

trained 3 days before the MCAO surgery. The mean duration (in seconds) on the device was recorded with three rotarod measurements 1 day before surgery. Test data are presented as the percentage of mean duration (three trials) on the rotarod compared with the internal baseline control (before surgery).[60]

Vibrissae stimulated forelimb placing test

Animals were held with the forelimbs hanging freely and the vibrissae were lightly stimulated with the edge of a bench top. Normal rats with an intact cortex will typically place the forepaw ipsilateral to the stimulated vibrissae on the bench top. Ten ipsilateral placing reactions were determined. Placing errors for each forelimb were computed as the percentage of missed placements per trial in all the experimental groups.[61]

Treadmill test

Rats were trained 20 minutes per day for 1 week to run on a motor driven treadmill at a speed of 6.3–6.4 m/minute with a slope of zero degrees. Forelimbs were placed on a moving belt facing away from the grid and induced to step in the direction opposite to the movement of the belt. The number of steps was recorded with three trials in all the experimental groups.

Statistical analysis

Statistical tests to determine differences between groups were performed with analysis of variance and a paired Student's *t*-test using IBM® SPSS version 14.0 (SPSS Inc, Chicago, IL). A P value of <0.05 was considered significant. Data are expressed as the mean ± standard deviation.

Results

Morphology and cell lineage of SVZ NPCs and confirmation of ischemic lesion

As mentioned, the NPCs were isolated from the SVZ and were then cultured for 2 weeks until transplantation (Figure 1A and B-c). The cultured SVZ NPCs differentiated after 2 weeks of culture (Figure 1A-c and A-d). The differentiated SVZ NPCs were stained predominantly with a neuronal cell marker (TUJ1) and an astrocyte marker (GFAP), with 4′,6-diamidino-2-phenylindole-labeled nuclei (Figure 1A-e and A-f). Rats were sacrificed 24 hours after surgery and TTC staining was performed to identify the brain lesion (Figure 1B-a). The lesion was also matched with magnetic resonance images (Figure 1B-b).

Ischemic lesion analysis

MCAO injury resulted in extensive infarction and cavitations along the ipsilateral cortex and striatum in the brain. To visualize and measure the damaged brain tissue, hematoxylin and eosin staining was performed for the experimental control groups (EC) and the SVZ NPCs alone, HL CNT-SVZ NPC, and HP CNT-SVZ NPC transplantation groups (Figure 2A) at 3, 5, and 8 weeks after MCAO injury. The brain injury area and volume was measured using an image analysis software program OPTIMUS 6.0 (OPTIMUS Corporation, Fort Collins, CO, version 3.5) (Figure 2B and C).

The infarct cyst volume and cyst area showed a significant decrease for the three transplantation groups compared with the EC groups. However, no significant difference was observed during infarct cyst volume and infarct cyst area analysis at 3 weeks and 5 weeks after MCAO injury (Figure 2). At 8 weeks, the three transplantation groups showed a significant reduction in the infarct cyst volume compared with the EC groups (Figure 2B). However, the HL CNT-SVZ NPC and HP CNT-SVZ NPC groups displayed better attenuation ($P < 0.05$) of the infarct cyst area compared with the SVZ NPCs alone group (Figure 2C). Importantly, the HP CNT-SVZ NPC transplants better compensated for the cavitations from MCAO injury compared with the other two transplantation groups after 3, 5, and 8 weeks of MCAO injury, but the values were not statistically significant among the groups (Figure 2B and C).

Neurological functional recovery tests

The animals were evaluated for their harmonic behavioral paradigm using an accelerating rotarod test until 8 weeks after MCAO injury. The three transplantation groups (SVZ NPCs alone, HL CNT-SVZ NPCs, and HP CNT-SVZ NPCs) displayed gradual improvement in the motor function – showing balance while holding the rotarod – compared to EC groups at all of the time periods; the values were statistically significant ($P < 0.05$) at 8 weeks. However, no significant divergence was observed among the three transplantation groups (Figure 3A).

The treadmill test results showed an improvement in rat walking ability in the three transplantation groups compared to the EC groups. The test results were found to be significant ($P < 0.05$) from 4 weeks until 8 weeks. Importantly, the HP CNT-SVZ NPC group showed better test scores compared with the other two transplantation groups, but the obtained scores were not significant between the groups (Figure 3B).

The sensory responses in all the experimental groups were tested with the vibrissae-stimulated forelimb placing test.

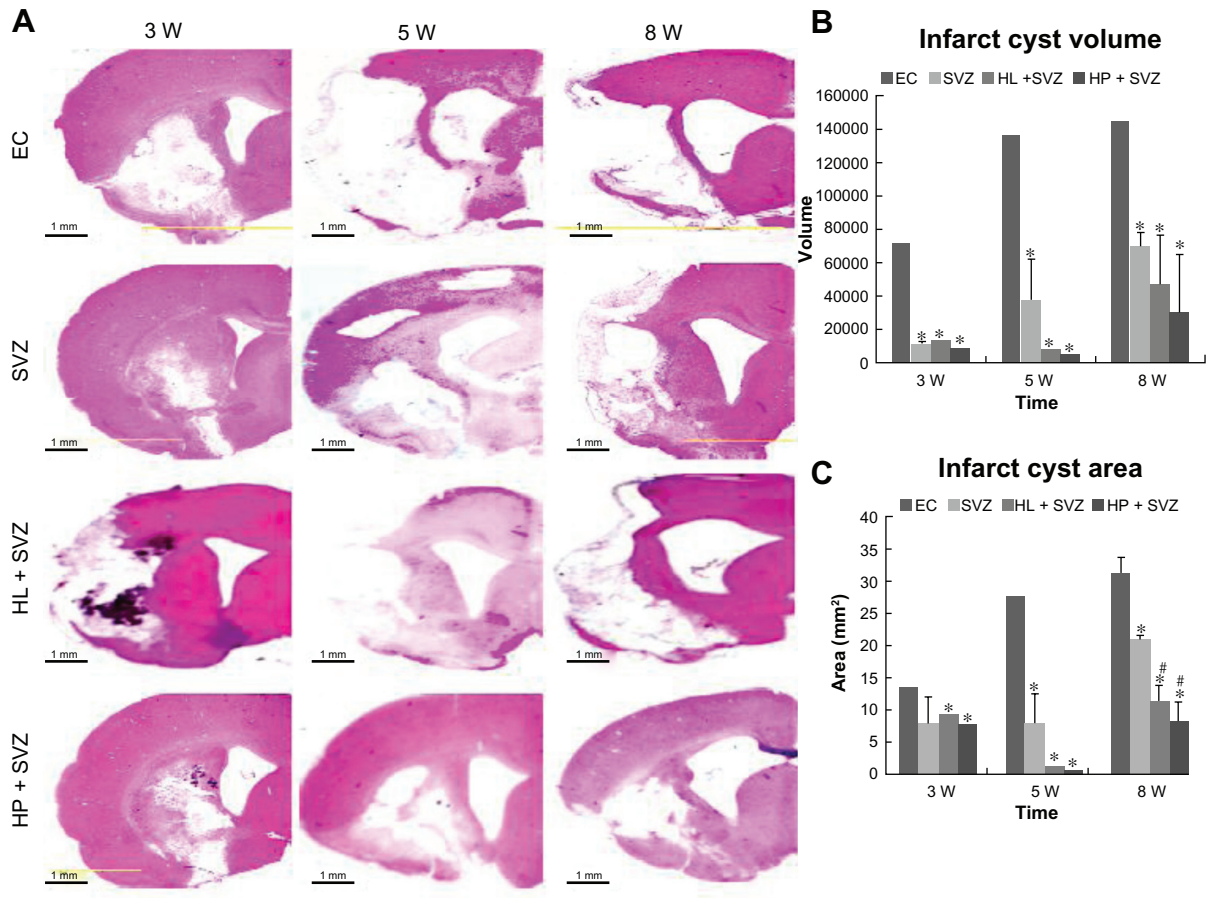

Figure 2 Quantification of infarct cyst volume and area by hematoxylin and eosin staining. Hydrophilic or hydrophobic carbon nanotubes were impregnated with subventricular zone neural progenitor cells and then transplanted into the injured brain tissue directly. Brain slices were stained with hematoxylin and eosin to (**A**) visualize and (**B** and **C**) measure the damaged tissue area of the brain. (**B**) Infarct cyst volumes and (**C**) infarct cyst area were measured with image-analysis software.
Notes: Scale bars = 1 mm; $^{*}P < 0.05$ compared to the experimental control group; $^{\#}P < 0.05$ compared to the subventricular zone neural progenitor cells alone group.
Abbreviations: EC, experimental control; HL + SVZ, hydrophilic carbon nanotubes impregnated with subventricular zone neural progenitor cells; HP + SVZ, hydrophobic carbon nanotubes impregnated with subventricular zone neural progenitor cells; SVZ, subventricular zone neural progenitor cells alone; W, weeks.

The three transplantation groups showed an improvement in the withdrawal reflex compared to the EC group. The values were found to be significant ($P < 0.05$) from 4 weeks until 8 weeks after which no significant divergence existed between the groups. In contrast, EC groups regained only about 50% of reflex after 8 weeks of injury (Figure 3C).

BrdU labeling and detection of stemness in CNTs impregnated with SVZ NPCs

As mentioned, the SVZ NPCs were prestained with BrdU and transplanted along with HL CNTs or HP CNTs into the MCAO injured rat brain. The BrdU-labeled SVZ NPCs migrated sparsely around the ischemic core region 3 weeks after transplantation (Figure 4A-a and B-a). Immunostaining results showed that the BrdU-labeled immunopositive cells were present around the corpus callosum (Figure 4A-c) for the HL CNT-SVZ NPC group, while no BrdU-labeled cells were found in the cortex region (Figure 4A-b) at 3 weeks after transplantation. BrdU-labeled SVZ NPCs were found migrating towards the striatum region of the brain (Figure 4A-d). Following MCAO, the transplantation of BrdU-labeled SVZ NPCs were concentrated along with the HP CNTs in the striatum region of the injured brain 3 weeks after MCAO injury (Figure 4B-c and B-d), but no BrdU-labeled immunopositive cells were found in the cortex region of the brain (Figure 4B-b).

Immunostaining was completed to detect the expression of nestin in HL CNT-SVZ NPCs and HP CNT-SVZ NPCs prestained with BrdU. Nestin immunopositive SVZ NPCs were observed around the HL CNTs and HP CNTs. Importantly, the total number of nestin immunopositive SVZ NPCs (brown stained) were found to be higher in the HP CNT-SVZ NPC group (Figure 4B-e) compared with the HL CNT-SVZ NPC group (Figure 4A-e).

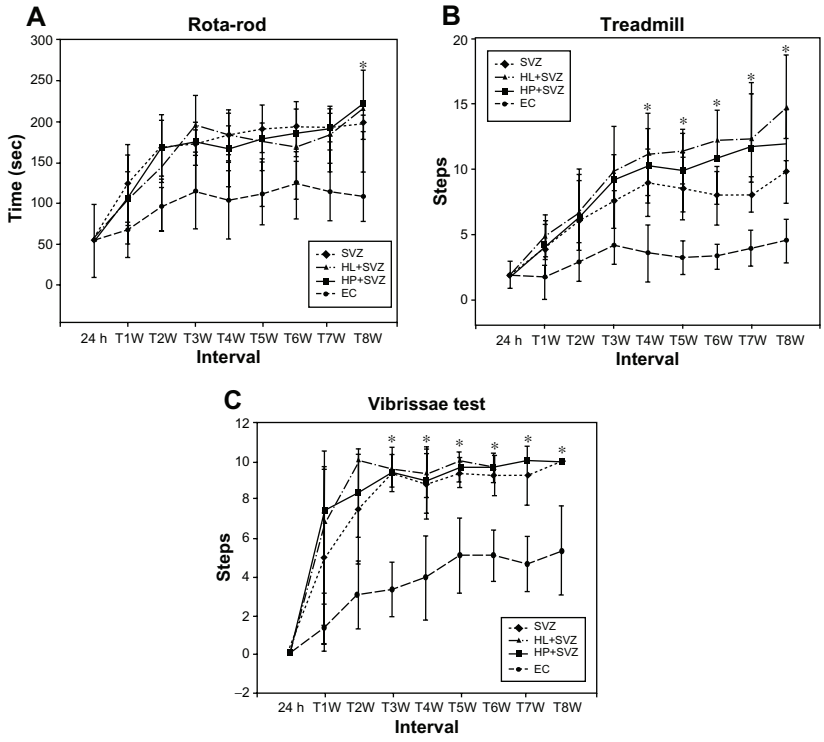

Figure 3 Analysis of behavior functional tests including (**A**) rotarod, (**B**) treadmill, and (**C**) vibrissae stimulated forelimb placing test after middle cerebral artery occlusion injury. Animals were subjected to injury alone, or injury-subjected animals were transplanted with subventricular zone neural progenitor cells alone, hydrophilic carbon nanotubes impregnated with subventricular zone neural progenitor cells, or hydrophobic carbon nanotubes impregnated with subventricular zone neural progenitor cells.
Notes: *$P < 0.05$ compared to the experimental control group.
Abbreviations: EC, experimental control; h, hours; HL + SVZ, hydrophilic carbon nanotubes impregnated with subventricular zone neural progenitor cells; HP + SVZ, hydrophobic carbon nanotubes impregnated with subventricular zone neural progenitor cells; SVZ, subventricular zone neural progenitor cells alone; W, weeks.

Migration and differentiation of the CNTs impregnated with SVZ NPCs

The migration and proliferation of the transplanted SVZ NPCs towards the injury site and scar area are important to compensate for the infarction caused by ischemic injury. DCX immunostaining was found in the SVZ NPCs alone (Figure 5B and F), HL CNT-SVZ NPC, and HP CNT SVZ NPC transplantation groups at 3 weeks and 5 weeks after MCAO injury (Figure 5C, D, G, and H). No DCX/BrdU double-stained immunopositive cells were found in the EC group (Figure 5A and E). Notably, the HP CNT-SVZ NPC group showed more DCX/BrdU double-stained immunopositive cells following MCAO injury compared with the other two transplantation groups at 5 weeks (Figure 5H). The transplanted cells migrated to the striatum and infarct scar regions.

Surface wettability of the CNTs impregnated with SVZ NPCs induced neurogenesis and functional synaptic formation

To ascertain whether the SVZ NPCs alone, HL CNT-SVZ NPC, and HP CNT-SVZ NPC transplants gave rise to neurons within the injury epicenter, immunostaining was performed for all the experimental groups with MAP2 at 5 weeks after ischemic injury (Figure 6). The MCAO injury resulted in tissue loss and MAP2 immunostaining results showed less expression of MAP2 immunopositive cells in the MCAO brain without SVZ NPC transplantation (EC) at 5 weeks after MCAO injury (Figure 6A). However, the three transplantation groups showed immunoreactivity with a MAP2 antibody and were found within the injury epicenter and around CNTs at 5 weeks after MCAO injury (Figure 6B–D). The HP CNT-SVZ NPC group showed higher interactions with SVZ NPCs and collectively spread around the ischemic injured brain to differentiate to become mature neurons at 5 weeks after transplantation (Figure 6D) compared with the SVZ NPC alone group (Figure 6B) and the HL CNT-SVZ NPC group (Figure 6C).

To examine the synapse formation, double-immunostaining for synaptophysin and TUJ1 – which reportedly correspond to synapses – were conducted after 5 weeks of transplantation in the HL CNT-SVZ NPC and HP CNT-SVZ NPC transplantation groups. At 5 weeks following transplantation, the HP CNT-SVZ NPC group was augmented with the formation of synapses to connect neuronal cells in the injured region

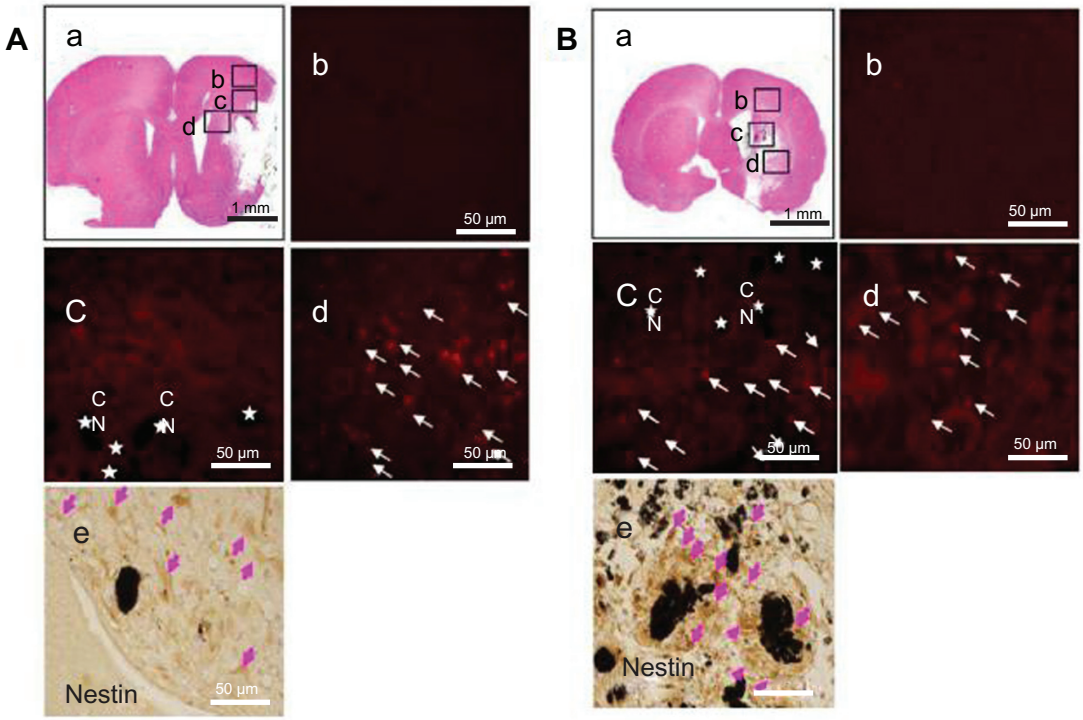

Figure 4 (**A**) Hydrophilic and (**B**) hydrophobic carbon nanotubes were impregnated with bromodeoxyuridine-stained (red; original magnification ×400) subventricular zone neural progenitor cells and transplanted onto the injury site after middle cerebral artery occlusion injury. The images show (a) the cross section of the injured brain stained with hematoxylin and eosin (where b□, c□, and d□ represent the cortex, corpus callosum, and striatum region of the brain, respectively), the migration of carbon nanotubes in the (b) cortex region, (c) corpus callosum, and (d) striatum region of the brain, and (e) diaminobenzidine staining results for nestin immunoreactivity (evidenced by brown-stained cells) 1 week after transplantation.

Notes: Carbon nanotubes appear black in the histological sections and are marked by ★. Arrows indicate bromodeoxyuridine-labeled subventricular zone neural progenitor cells. Original magnification for immunohistological staining was ×800. Scale bars = 50 μm.

Abbreviation: CN, carbon nanotubes.

(Figure 6F). However, no such phenomenon was observed in the HL CNT-SVZ NPC group (Figure 6E). These results demonstrated that the HP CNT-SVZ NPC transplants exhibited the characteristics of functional neurons with a large degree of synapse formation.

Surface wettability of CNTs impregnated with SVZ NPCs decreases astrogenesis

Reactive astrogliosis is one of the key components of the cellular response to CNS injury and is considered to be a major impediment to axonal regeneration. Immunohistochemistry was performed for all the experimental groups to examine gliogenesis by checking the expression of astrocytes (GFAP) and proliferating cells (Ki67) at 5 weeks after MCAO injury. The EC group showed high immunoreactivity with the GFAP and KI67 antibody showing that gliogenesis was activated following MCAO injury (Figure 7A). GFAP positive cells were found in the three transplantation groups. The transplantation of SVZ NPCs alone showed a low number of GFAP and Ki67 positive cells (Figure 7B), but the number was higher when compared with the HL CNT-SVZ NPC and HP CNT-SVZ NPC groups (Figure 7C and D). The HP CNT-SVZ NPC transplants showed better attenuation of GFAP expression at 5 weeks after MCAO injury compared with the other experimental groups (Figure 7D). A similar pattern of GFAP expression was seen with the diaminobenzidine staining depicting that HP CNT-SVZ NPC transplants (Figure 7F) decreased astrocytes formation compared with HL CNT-SVZ NPC transplants (Figure 7E) at 5 weeks after MCAO injury. Impressively, the results obtained suggest that the activation of gliogenesis following MCAO injury was significantly abolished in the HP CNT-SVZ NPC transplants, thus, demonstrating the high compatibility of HP CNTs against brain injuries.

Surface wettability of CNTs impregnated with SVZ NPCs transplantation decreased the inflammatory responses after ischemic injury

To distinguish microglia activation during inflammation due to brain injury, immunostaining was performed with OX-42 at 1, 3, and 5 weeks after MCAO injury in all the experimental

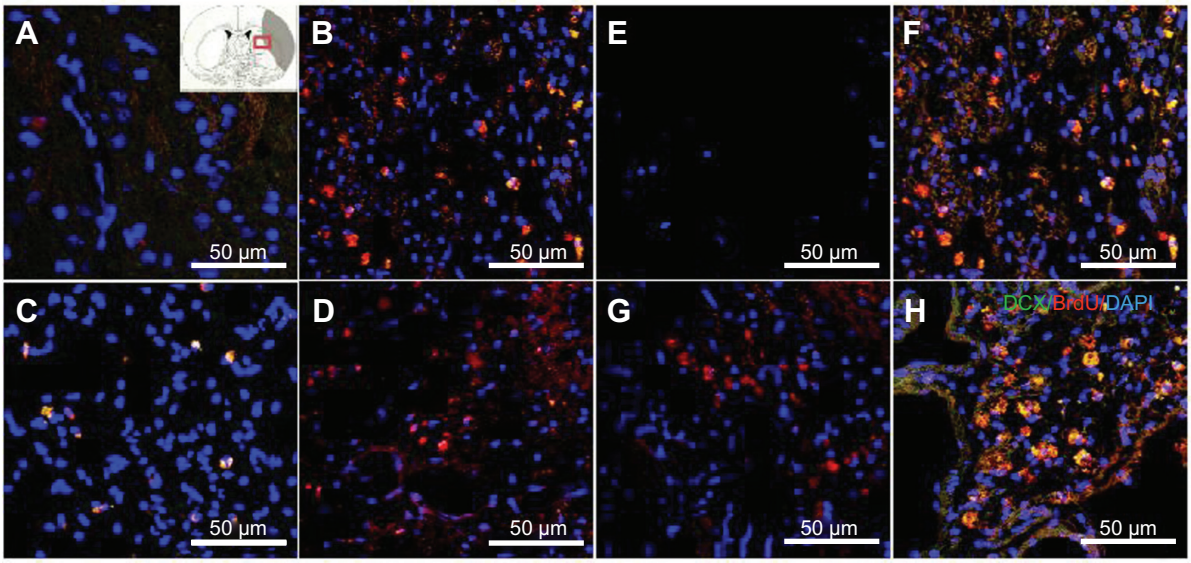

Figure 5 Doublecortin and bromodeoxyuridine staining was performed to detect the migrating exogenous subventricular zone neural progenitor cells in the hydrophilic or hydrophobic carbon nanotubes transplantation groups (**A** and **D**) 3 weeks or (**E** and **H**) 5 weeks after middle cerebral artery occlusion injury. The images show (**A** and **E**) the experimental control group (without subventricular zone neural progenitor cell transplantation), (**B** and **F**) injury-subjected rats transplanted with subventricular zone neural progenitor cells, (**C** and **G**) injury-subjected rats transplanted with hydrophilic carbon nanotubes impregnated with subventricular zone neural progenitor cells, and (**D** and **H**) injury-subjected rats transplanted with hydrophobic carbon nanotubes impregnated with subventricular zone neural progenitor cells.
Notes: Doublecortin and bromodeoxyuridine double positive immunostained cells are indicated by yellow. Scale bars = 50 μm.
Abbreviations: BrdU, bromodeoxyuridine; DAPI, 4′,6-diamidino-2-phenylindole; DCX, doublecortin.

groups (Figure 8). Immunostaining results provided evidence of a less activated expression of microglia in the SVZ NPCs alone (Figure 8D–F), HP CNT-SVZ NPC, and HL CNT-SVZ NPC transplantation groups (Figure 8G–L) compared to EC groups (Figure 8A–C) at 1 week and 3 weeks after MCAO injury (Figure 8A and B). The activation was gradually diminished at 5 weeks in all the experimental groups. For both the HL CNT-SVZ NPC and HP CNT-SVZ NPC groups, less activated microglia was observed compared to the SVZ NPCs alone group. Importantly, the number of OX-42 immunopositive cells were lower in the HP CNT-SVZ NPC group compared with the other experimental groups at 1, 3, or 5 weeks after MCAO injury.

Discussion

If designed correctly, biomaterials can provide a new cytoskeletal scaffold for restoring neural tissue function for numerous neurological disorders and injuries including stroke.[62,63] Recently, several biomaterials have given hope to develop powerful tools for supporting NPC transplantation to repair damage in the CNS. While popular synthetic polymers, such as poly(D,L-lactide-co-glycolide) and poly(L-lactide), have been widely studied for various tissue engineering applications, they lack the necessary electrical properties for neural applications.[1] In contrast, CNTs are electrically active and can be formulated to mimic the nanoscale features of natural neurological tissues.[64] Compared to conventional carbon tubes, CNTs also possess unique mechanical properties such as high strength to weight ratios, high conductivity, and unique surface properties for regenerating neural networks.[64] Neurons deposited on CNTs have demonstrated a significant increase in formulating spontaneous postsynaptic currents,[44] and mesenchymal stem cells and NSCs grown on CNT arrays increase their potential for proliferation and differentiation.[50] However, the use of CNTs in vivo to promote stem cell functions for reversing neural damage has not been widely studied to date. The present study presents the first evidence of their promise towards differentiating NSCs to neurons to promote damaged neural tissue healing.

Cell adhesion on artificial materials is affected by their surface properties such as wettability, roughness, surface charge, and chemical functionalities.[65] Diverse properties of CNTs can help overcome the restriction and limitation of stem cell therapy. Overall, carbon nanomaterials could be used for promoting stem cells and NPC functions in an injured brain. In a previous study, it was demonstrated that CNTs assisted in the proliferation of mesenchymal stem cells and aided in the differentiation of NSCs in cell culture systems in vitro.[50] Therefore, the present study was conducted to prove whether HP CNTs or HL CNTs positively and selectively interacted with NPCs in the ischemic injured brain to assist NPCs to differentiate to become mature neural cells.

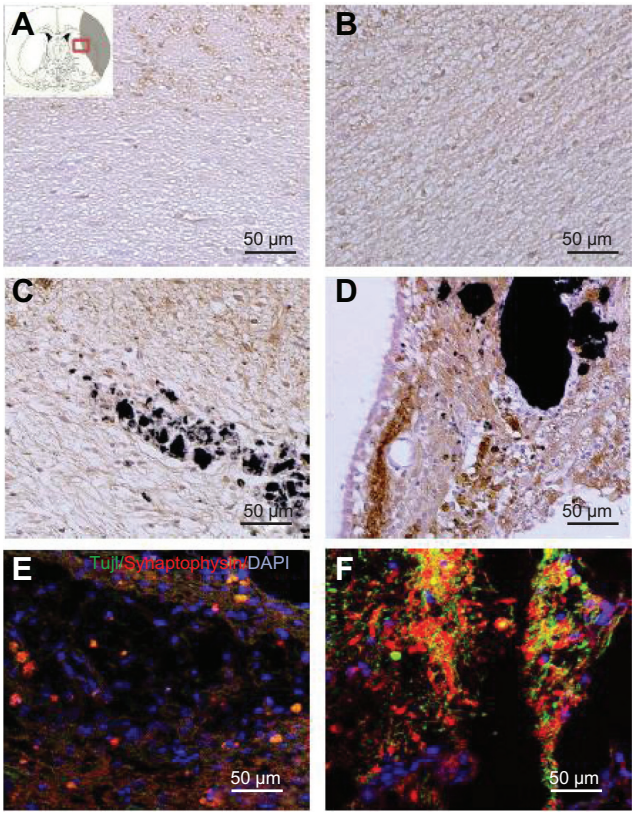

Figure 6 Images showing the neurogenesis and synapse formation based on the wettability of carbon nanotubes following middle cerebral artery occlusion injury. Microtubule-like associated protein 2 immunostaining was performed in (**A**) the experimental control group (without subventricular zone neural progenitor cell transplantation) and (**B**) the subventricular zone neural progenitor cells alone, (**C**) hydrophilic carbon nanotubes impregnated with subventricular zone neural progenitor cell, and (**D**) hydrophobic carbon nanotubes impregnated with subventricular zone neural progenitor cell transplantation groups at 5 weeks after middle cerebral artery occlusion injury. Synaptophysin (a synapse marker; red) and TUJ1 (a neuronal marker; green) – which reportedly correspond to synapses – immunostaining was carried out at 5 weeks after transplantation with (**E**) hydrophilic and (**F**) hydrophobic carbon nanotubes impregnated with subventricular zone neural progenitor cells.
Note: Scale bars = 50 μm.
Abbreviation: DAPI, 4′,6-diamidino-2-phenylindole.

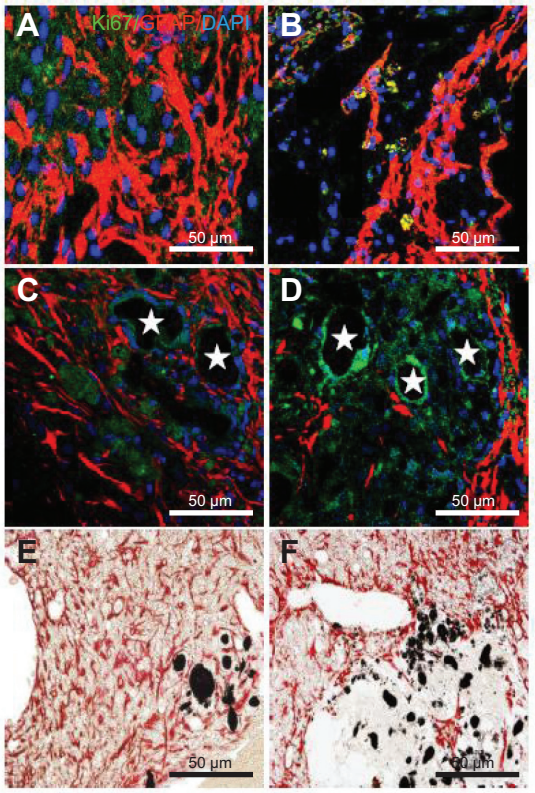

Figure 7 Immunostaining was performed with glial fibrillary acidic protein (astrocyte marker; red), and Ki67 (proliferation marker) in (**A**) the experimental control group (without subventricular zone neural progenitor cell transplantation) and (**B**) the subventricular zone neural progenitor cells alone, (**C**) hydrophilic carbon nanotubes impregnated with subventricular zone neural progenitor cell, and (**D**) hydrophobic carbon nanotubes impregnated with subventricular zone neural progenitor cell transplantation groups 5 weeks after middle cerebral artery occlusion injury. Glial fibrillary immunopositive cells are stained red and Ki67 immunopositive cells are stained green. The diaminobenzidine staining results for glial fibrillary acidic protein immunoreactivity (evidenced by brown-stained cells) in (**E**) hydrophilic and (**F**) hydrophobic carbon nanotubes impregnated with subventricular zone neural progenitor cells are also shown.
Notes: Carbon nanotubes appear black in the histological sections and are marked by ★. Original magnification for immunohistological staining was ×800. Bar = 50 μm.
Abbreviation: DAPI, 4′,6-diamidino-2-phenylindole.

Results demonstrated that the different wettability properties of CNTs influenced NPC differentiation into neurons and glial scar tissue formation. In particular, this study demonstrated for the first time that HP CNTs outperformed HL CNTs, which outperformed SVZ NPCs alone or no treatment at all (EC). In this manner, CNTs can be structurally supportive to the long-term survival and differentiation of exogenous SVZ NPCs. The functional recovery of rats when using SVZ NPCs alone, HP CNP-SVZ NPC, or HL CNT-SVZ NPC transplants was tested by rotarod, treadmill, and vibrissae-stimulated forelimb placing tests. The SVZ NPCs alone, HL CNT-SVZ NPC, and HP CNT-SVZ NPC transplants functionally improved rat function more than lesion-control groups (EC) for all the recovery tests performed. There was no significant difference among the SVZ NPCs alone, HL CNT-SVZ NPC, or HP CNT-SVZ NPC groups in the rotarod, treadmill, and vibrissae-stimulated forelimb placing tests. However, the HP CNT-SVZ NPC groups showed better test scores compared with the HL CNT-SVZ NPC and SVZ NPCs alone groups and, thus, more studies investigating this are needed.

Teng et al[32] in 2002 demonstrated that rats with lesioned spinal cords implanted with NSC constructs improved recovery of hindlimb locomotor functions compared with empty scaffolds and cells. They claimed that the recovery was attributed to a reduction in tissue loss from secondary injury processes, diminished glial scarring, and, to a certain extent, reestablishment of axonal connectivity across the lesion supported by the NSCs scaffold construct.[1,32] Also, another

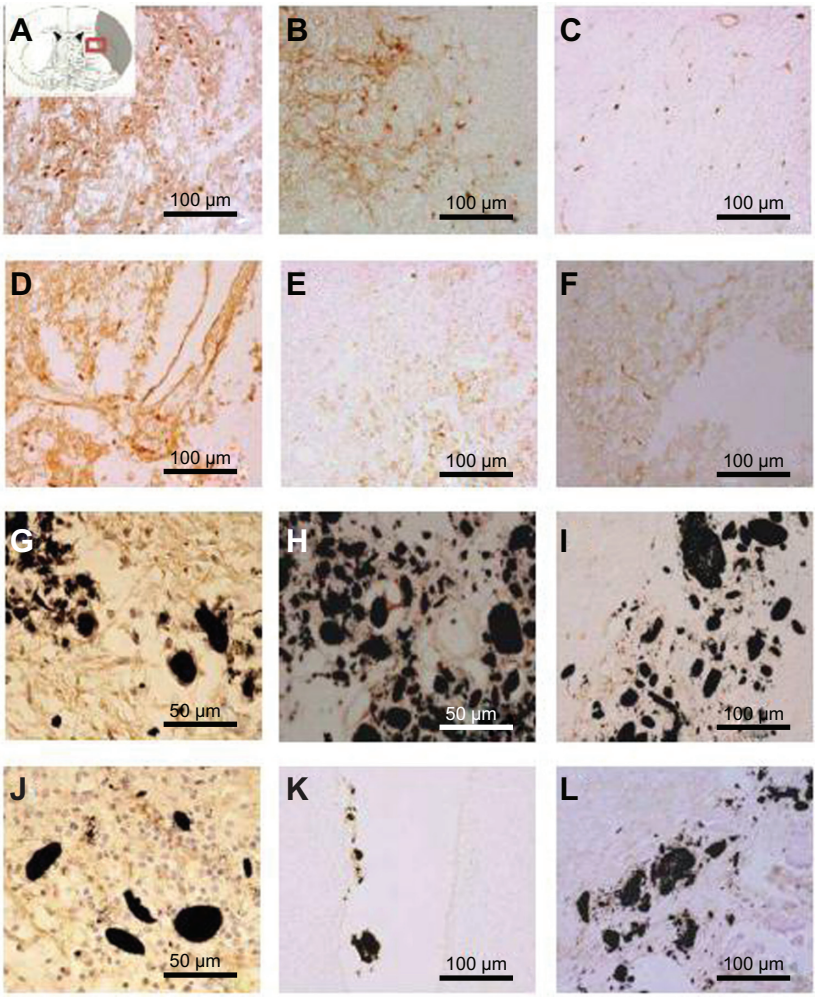

Figure 8 Immunostaining was performed with CD11b/c (OX-42) to reveal the expression of activated microglial cells (evidenced by brown-stained cells) (**A**, **D**, **G**, **J**) 1 week, (**B**, **E**, **H**, **K**) 3 weeks, and (**C**, **F**, **I**, **L**) 5 weeks after middle cerebral artery occlusion injury. The experimental groups included (**A**–**C**) the experimental control group (without subventricular zone neural progenitor cell transplantation) and the (**D**–**F**) subventricular zone neural progenitor cells alone, (**G**–**I**) hydrophilic carbon nanotubes impregnated with subventricular zone neural progenitor cell, and (**J**–**L**) hydrophobic carbon nanotubes impregnated with subventricular zone neural progenitor cell transplantation groups.
Notes: Scale bars = 100 μm. Carbon nanotubes appear black.

study in hypoxia–ischemia injury models reported diminished unilateral rotation because the synthetic ECM helped bridge large brain lesions and foster the creation of new tissues by impregnating NSCs.[33] In these studies, they did not study the relationship between the different wettability of nanomaterials and functional recovery of animals. As they stated, the synthetic scaffolds or CNTs might provide a platform to help recover the injured brain tissue. Even though behavior recovery was not significantly distinctive between the three transplantation groups here, the diminished infarction cavity improved effectiveness of the HP CNT-SVZ NPCs over HL CNT-SVZ NPCs and SVZ NPCs alone.

A study reported that exogenous stem cells were highly migratory, were attracted towards ischemic regions, and differentiated into neuronal cells to refill a cavity.[66] The highly conductive nature of CNTs is promising towards promoting SVZ NPCs differentiation. That is, it is plausible that immediately upon implantation, CNTs conduct electricity from the healthy parts of the brain and this conduction aids SVZ NPCs differentiation into neurons. Although the mechanisms of such differentiation were not elucidated here, the HP CNTs might have different conduction properties compared to the HL CNTs which may influence their agglomeration and overall ability to differentiate NPCs into neurons.[52,67] Based on these hypotheses, immunolabeling with BrdU and nestin was completed to characterize the SVZ NPCs at 3 weeks following transplantation. The staining results showed that the rate of SVZ NPCs spreading was similar in the core striatum both in HL CNT-SVZ NPC and HP CNT-SVZ NPC groups. The HP CNTs interacted with SVZ NPCs which collectively spread around the ischemic injured brain and helped the SVZ NPCs residing in the

brain to differentiate to become mature neurons 3 weeks or 5 weeks after transplantation. In terms of promoting SVZ NPCs differentiation into neurons and decreasing glial scar tissue formation, the SVZ NPCs alone, HL CNT-SVZ NPC, and HP CNT-SVZ NPC transplants increased the number of MAP2 positive cells and decreased the number of GFAP positive cells, but the HP CNT-SVZ NPC group had better results compared with other experimental groups at 3 weeks or 5 weeks after MCAO injury.

Although controversial, astrocytes have been correlated with the formation of inhibitory glial scar tissue. Thus, a reduction in astrocyte growth following injury is believed to be desirable.[32] These distinctive results were related to CNT wettability in the current study in which HP CNTs decreased glial scar tissue the most. A study demonstrated decreased numbers of macrophages along aligned CNTs on polycarbonate urethane.[51] In a previous study,[68] while CNTs were functionalized to attach either electrostatically or covalently to deoxyribonucleic acid and ribonucleic acid, the remaining unfunctionalized and HP portions of the CNTs can be attracted to the HP regions of the cell. This hydrophobicity explains the nonspecific binding between nanotubes and proteins and in addition, they can be functionalized with bioactive proteins to help cross the cellular membrane.[68] Kim et al proved that wettable surfaces could regulate c-fos, c-myc, and p53 messenger ribonucleic acid expression of human bone marrow stromal cells suggesting that biomaterial wettability could alter messenger ribonucleic acid expression levels of cells to control cell proliferation.[28]

The hydrophobicity of a biomaterial surface is directly related to cell adhesion to biomaterials since the cells adhere to the surface through binding of their adhesion receptors to adhesion ligands (ie, proteins) absorbed to the surface, and adhesion ligand adsorption to the surface depends on surface wettability which determines the conformation of the proteins on the surface.[67] Here, most of the primary cultured neurons grew on HP CNT arrays. At HP CNT surfaces, specific proteins such as laminin, vitronectin, and fibronectin[53–55] that mediate primary cultured neuron attachment and extension of their axons may add or subtract to the surface tension between the cell and nanostructured surfaces. It is clearly possible that the same proactive properties that promoted primary neurons in that in vitro study are promoting stem cell differentiation in the current in vivo study. These results (attraction of protein adsorption from neural tissue) may have caused the HP CNTs not to migrate in the brain which would increase their ability to serve as "anchors" for SVZ NPC differentiation at the site of stroke damage. In addition, previous research has suggested that these same CNTs increase adsorption of laminin, a key protein for promoting NPC differentiation into neurons.[48]

To explain the functional recovery of animals, the migration to the injury site and synaptic formation of exogenous SVZ NPCs were investigated here with immunohistochemistry. HL CNT-SVZ NPC and HP CNT-SVZ NPC transplants showed early migration of SVZ NPCs to the injury core striatum. But, DCX immunoreactivity was higher in the HP CNT-SVZ NPC group compared with the HL CNT-SVZ NPC and SVZ NPCs alone groups. For structural integration of the brain, the CNTs probably facilitated not only migration of SVZ NPCs but also neuronal connectivity. At 5 weeks following injury, HP CNT-SVZ NPC transplantation helped the formation of synapses to connect neuronal cells to the host tissues. However, synapse formation was not seen at 1 week or 3 weeks after transplantation (data not shown). These results proved that the wettability of CNTs influenced differentiated SVZ NPCs to exhibit the characteristics of functional neurons and degree of synapse formation.

Earlier it was reported that NPCs alone (without CNTs) did not stay in the damaged portion of the brain, but rather they migrated toward healthy portions of the brain after transplantation.[40] Using CNTs alone, little restoration of the infarct cavity was observed in the injured brain.[33] An understanding of the feasibility of implanting stem cells, their behavior of migration in response to lesions induced in brain tissues, and the mechanism of their in vivo differentiation into neighboring neural cells is essential for developing and refining stem cell transplantation strategies for the repair of damaged nervous system tissue.[62,63,69] The current study clearly demonstrates that nanosized carbon materials possessing different surface energies can be utilized as novel biocompatible materials with strong potential for healing damaged neural tissue. A better understanding of the interactions of HP CNTs and HL CNTs with stem cells at the molecular level may help to further such efforts and help transplanted NPCs reside and differentiate into neurons in injured brains.

Conclusion

This current investigation revealed that CNTs impregnated with SVZ NPCs could heal stroke damaged neural tissue in a rodent model. Compared to the EC groups, results of this in vivo study provided evidence that CNTs helped the differentiation of SVZ NPCs into viable, functioning neurons that might reestablish electrical activity in damaged neural tissue. Also, these results proved that HP CNTs

outperformed HL CNTs and efficiently differentiated SVZ NPCs to become migrating functional neurons with synapse formation. Overall, the animals transplanted with SVZ NSCs alone and CNTs impregnated with SVZ NPCs showed functional recovery, but the results were better with CNTs. Such data highlights the promising role that CNTs may play in healing brain damage that may occur due to a number of neuropathological situations (eg, stroke, Parkinson's disease, and Huntington's disease).

Acknowledgments

This research was partially supported by the Basic Science Research Program through the National Research Foundation of Korea funded by the Ministry of Education, Science, and Technology (KRF-2007-531-E00003) and "System IC 2010" project of Korean Ministry of Commerce, Industry, and Energy. The authors would like to thank the Herman Foundation and National Science Foundation for funding.

Disclosure

The authors report no conflicts of interest in this work.

References

1. Chai C, Leong KW. Biomaterials approach to expand and direct differentiation of stem cells. *Mol Ther*. 2007;15(3):467–480.
2. Ma W, Fitzgerald W, Liu QY, et al. CNS stem and progenitor cell differentiation into functional neuronal circuits in three-dimensional collagen gels. *Exp Neurol*. 2004;190(2):276–288.
3. Ruoslahti E. Stretching is good for a cell. *Science*. 1997;276(5317):1345–1346.
4. Discher DE, Janmey P, Wang YL. Tissue cells feel and respond to the stiffness of their substrate. *Science*. 2005;310(5751):1139–1143.
5. Baier RE, Meyer AE, Natiella JR, Natiella RR, Carter JM. Surface properties determine bioadhesive outcomes: methods and results. *J Biomed Mater Res*. 1984;18(4):327–355.
6. Engler AJ, Sen S, Sweeney HL, Discher DE. Matrix elasticity directs stem cell lineage specification. *Cell*. 2006;126(4):677–689.
7. Weiss P. Experiments on cell and axon orientation in vitro; the role of colloidal exudates in tissue organization. *J Exp Zool*. 1945;100:353–386.
8. Curtis AS, Varde M. Control of cell behavior: topological factors. *J Natl Cancer Inst*. 1964;33:15–26.
9. Curtis A, Wilkinson C. Topographical control of cells. *Biomaterials*. 1997;18(24):1573–1583.
10. Curtis A, Wilkinson C. New depths in cell behaviour: reactions of cells to nanotopography. *Biochem Soc Symp*. 1999;65:15–26.
11. Recknor JB, Sakaguchi DS, Mallapragada SK. Directed growth and selective differentiation of neural progenitor cells on micropatterned polymer substrates. *Biomaterials*. 2006;27(22):4098–4108.
12. Yang F, Murugan R, Wang S, Ramakrishna S. Electrospinning of nano/micro scale poly(L-lactic acid) aligned fibers and their potential in neural tissue engineering. *Biomaterials*. 2005;26(15):2603–2610.
13. Oliva AA Jr, James CD, Kingman CE, Craighead HG, Banker GA. Patterning axonal guidance molecules using a novel strategy for microcontact printing. *Neurochem Res*. 2003;28(11):1639–1648.
14. Estes BT, Gimble JM, Guilak F. Mechanical signals as regulators of stem cell fate. *Curr Top Dev Biol*. 2004;60:91–126.
15. McBeath R, Pirone DM, Nelson CM, Bhadriraju K, Chen CS. Cell shape, cytoskeletal tension, and RhoA regulate stem cell lineage commitment. *Dev Cell*. 2004;6(4):483–495.
16. Weiss L. The adhesion of cells. *Int Rev Cytol*. 1960;9:187–225.
17. Kaelble DH, Moacanin J. Surface energetics analysis of artificial blood substitutes. *Med Biol Eng Comput*. 1979;17(5):593–601.
18. Grinnell F. Cellular adhesiveness and extracellular substrata. *Int Rev Cytol*. 1978;53:65–144.
19. Absolom DR, Hawthorn LA, Chang G. Endothelialization of polymer surfaces. *J Biomed Mater Res*. 1988;22(4):271–285.
20. Schleicher I, Parker A, Leavesley D, Crawford R, Upton Z, Xiao Y. Surface modification by complexes of vitronectin and growth factors for serum-free culture of human osteoblasts. *Tissue Eng*. 2005;11(11–12):1688–1698.
21. Hamilton DW, Riehle MO, Monaghan W, Curtis AS. Chondrocyte aggregation on micrometric surface topography: a time-lapse study. *Tissue Eng*. 2006;12(1):189–199.
22. Kim TG, Park TG. Biomimicking extracellular matrix: cell adhesive RGD peptide modified electrospun poly(D,L-lactic-co-glycolic acid) nanofiber mesh. *Tissue Eng*. 2006;12(2):221–233.
23. van Wachem PB, Beugeling T, Feijen J, Bantjes A, Detmers JP, van Aken WG. Interaction of cultured human endothelial cells with polymeric surfaces of different wettabilities. *Biomaterials*. 1985;6(6):403–408.
24. van Wachem PB, Hogt AH, Beugeling T, et al. Adhesion of cultured human endothelial cells onto methacrylate polymers with varying surface wettability and charge. *Biomaterials*. 1987;8(5):323–328.
25. Kishida A, Iwata H, Tamada Y, Ikada Y. Cell behaviour on polymer surfaces grafted with non-ionic and ionic monomers. *Biomaterials*. 1991;12(8):786–792.
26. Lee JH, Khang G, Lee JW, Lee HB. Interaction of different types of cells on polymer surfaces with wettability gradient. *J Colloid Interface Sci*. 1998;205(2):323–330.
27. Lee JH, Lee JW, Khang G, Lee HB. Interaction of cells on chargeable functional group gradient surfaces. *Biomaterials*. 1997;18(4):351–358.
28. Kim MS, Shin YN, Cho MH, et al. Adhesion behavior of human bone marrow stromal cells on differentially wettable polymer surfaces. *Tissue Eng*. 2007;13(8):2095–2103.
29. Wilson CJ, Clegg RE, Leavesley DI, Pearcy MJ. Mediation of biomaterial–cell interactions by adsorbed proteins: a review. *Tissue Eng*. 2005;11(1–2):1–18.
30. Lin JC, Tseng SM. Surface characterization and platelet adhesion studies on polyethylene surface with hirudin immobilization. *J Mater Sci Mater Med*. 2001;12(9):827–832.
31. Akerud P, Canals JM, Snyder EY, Arenas E. Neuroprotection through delivery of glial cell line-derived neurotrophic factor by neural stem cells in a mouse model of Parkinson's disease. *J Neurosci*. 2001;21(20):8108–8118.
32. Teng YD, Lavik EB, Qu X, et al. Functional recovery following traumatic spinal cord injury mediated by a unique polymer scaffold seeded with neural stem cells. *Proc Natl Acad Sci U S A*. 2002;99(5):3024–3029.
33. Park KI, Teng YD, Snyder EY. The injured brain interacts reciprocally with neural stem cells supported by scaffolds to reconstitute lost tissue. *Nat Biotechnol*. 2002;20(11):1111–1117.
34. Borlongan CV, Tajima Y, Trojanowski JQ, Lee VM, Sanberg PR. Cerebral ischemia and CNS transplantation: differential effects of grafted fetal rat striatal cells and human neurons derived from a clonal cell line. *Neuroreport*. 1998;9(16):3703–3709.
35. Ourednik V, Ourednik J, Flax JD, et al. Segregation of human neural stem cells in the developing primate forebrain. *Science*. 2001;293(5536):1820–1824.
36. Steindler DA. Neural stem cells, scaffolds, and chaperones. *Nat Biotechnol*. 2002;20(11):1091–1093.

37. Lois C, Alvarez-Buylla A. Proliferating subventricular zone cells in the adult mammalian forebrain can differentiate into neurons and glia. *Proc Natl Acad Sci U S A*. 1993;90(5):2074–2077.
38. Snyder EY, Taylor RM, Wolfe JH. Neural progenitor cell engraftment corrects lysosomal storage throughout the MPS VII mouse brain. *Nature*. 1995;374(6520):367–370.
39. Martinez-Serrano A, Bjorklund A. Protection of the neostriatum against excitotoxic damage by neurotrophin-producing, genetically modified neural stem cells. *J Neurosci*. 1996;16(15):4604–4616.
40. Snyder EY, Yoon C, Flax JD, Macklis JD. Multipotent neural precursors can differentiate toward replacement of neurons undergoing targeted apoptotic degeneration in adult mouse neocortex. *Proc Natl Acad Sci U S A*. 1997;94(21):11663–11668.
41. Gage FH. Cell therapy. *Nature*. 1998;392(Suppl 6679):18–24.
42. Bellamkonda R, Ranieri JP, Bouche N, Aebischer P. Hydrogel-based three-dimensional matrix for neural cells. *J Biomed Mater Res*. 1995;29(5):663–671.
43. Woerly S, Petrov P, Sykova E, Roitbak T, Simonova Z, Harvey AR. Neural tissue formation within porous hydrogels implanted in brain and spinal cord lesions: ultrastructural, immunohistochemical, and diffusion studies. *Tissue Eng*. 1999;5(5):467–488.
44. Lovat V, Pantarotto D, Lagostena L, et al. Carbon nanotube substrates boost neuronal electrical signaling. *Nano Lett*. 2005;5(6):1107–1110.
45. Johansson F, Carlberg P, Danielsen N, Montelius L, Kanje M. Axonal outgrowth on nano-imprinted patterns. *Biomaterials*. 2006;27(8):1251–1258.
46. Elias KL, Price RL, Webster TJ. Enhanced functions of osteoblasts on nanometer diameter carbon fibers. *Biomaterials*. 2002;23(15):3279–3287.
47. Price RL, Waid MC, Haberstroh KM, Webster TJ. Selective bone cell adhesion on formulations containing carbon nanofibers. *Biomaterials*. 2003;24(11):1877–1887.
48. McKenzie JL, Waid MC, Shi R, Webster TJ. Decreased functions of astrocytes on carbon nanofiber materials. *Biomaterials*. 2004;25(7–8):1309–1317.
49. Price RL, Ellison K, Haberstroh KM, Webster TJ. Nanometer surface roughness increases select osteoblast adhesion on carbon nanofiber compacts. *J Biomed Mater Res A*. 2004;70(1):129–138.
50. Nho Y, Kim JY, Khang D, Webster TJ, Lee JE. Adsorption of mesenchymal stem cells and cortical neural stem cells on carbon nanotube/polycarbonate urethane. *Nanomedicine (Lond)*. 2010;5(3):409–417.
51. Kim JY, Khang D, Lee JE, Webster TJ. Decreased macrophage density on carbon nanotube patterns on polycarbonate urethane. *J Biomed Mater Res A*. 2009;88(2):419–426.
52. Lee JE, Khang D, Webster TJ. Stem cell impregnated carbon nanotubes nanofibers for healing damaged neural tissue. *Mater Res Soc Symp Proc*. 2006;915:R01–R07.
53. Grinnell F, Feld MK. Fibronectin adsorption on hydrophilic and hydrophobic surfaces detected by antibody binding and analyzed during cell adhesion in serum-containing medium. *J Biol Chem*. 1982;257(9):4888–4893.
54. Horbett TA, Schway MB. Correlations between mouse 3T3 cell spreading and serum fibronectin adsorption on glass and hydroxyethylmethacrylate-ethylmethacrylate copolymers. *J Biomed Mater Res*. 1988;22(9):763–793.
55. Steele JG, Johnson G, Underwood PA. Role of serum vitronectin and fibronectin in adhesion of fibroblasts following seeding onto tissue culture polystyrene. *J Biomed Mater Res*. 1992;26(7):861–884.
56. Lee JE, Yenari MA, Sun GH, et al. Differential neuroprotection from human heat shock protein 70 overexpression in in vitro and in vivo models of ischemia and ischemia-like conditions. *Exp Neurol*. 2001;170(1):129–139.
57. Yenari MA, Palmer JT, Sun GH, de Crespigny A, Mosely ME, Steinberg GK. Time-course and treatment response with SNX-111, an N-type calcium channel blocker, in a rodent model of focal cerebral ischemia using diffusion-weighted MRI. *Brain Res*. 1996;739(1–2):36–45.
58. Windle V, Corbett D. Fluoxetine and recovery of motor function after focal ischemia in rats. *Brain Res*. 2005;1044(1):25–32.
59. Kim JH, Yenari MA, Giffard RG, Cho SW, Park KA, Lee JE. Agmatine reduces infarct area in a mouse model of transient focal cerebral ischemia and protects cultured neurons from ischemia-like injury. *Exp Neurol*. 2004;189(1):122–130.
60. Chen J, Li Y, Wang L, Lu M, Zhang X, Chopp M. Therapeutic benefit of intracerebral transplantation of bone marrow stromal cells after cerebral ischemia in rats. *J Neurol Sci*. 2001;189(1–2):49–57.
61. Napieralski JA, Banks RJ, Chesselet MF. Motor and somatosensory deficits following uni- and bilateral lesions of the cortex induced by aspiration or thermocoagulation in the adult rat. *Exp Neurol*. 1998;154(1):80–88.
62. Limke TL, Rao MS. Neural stem cells in aging and disease. *J Cell Mol Med*. 2002;6(4):475–496.
63. Srivastava AS, Shenouda S, Mishra R, Carrier E. Transplanted embryonic stem cells successfully survive, proliferate, and migrate to damaged regions of the mouse brain. *Stem Cells*. 2006;24(7):1689–1694.
64. Harrison BS, Atala A. Carbon nanotube applications for tissue engineering. *Biomaterials*. 2007;28(2):344–353.
65. Ratner BD. *Biomaterials Science: An Introduction to Materials in Medicine*. San Diego: Academic Press; 1996.
66. Chang YC, Shyu WC, Lin SZ, Li H. Regenerative therapy for stroke. *Cell Transplant*. 2007;16(2):171–181.
67. Vermeer AW, Giacomelli CE, Norde W. Adsorption of IgG onto hydrophobic teflon. Differences between the F(ab) and F(c) domains. *Biochim Biophys Acta*. 2001;1526(1):61–69.
68. Chen RJ, Bangsaruntip S, Drouvalakis KA, et al. Noncovalent functionalization of carbon nanotubes for highly specific electronic biosensors. *Proc Natl Acad Sci U S A*. 2003;100(9):4984–4989.
69. Arvidsson A, Collin T, Kirik D, Kokaia Z, Lindvall O. Neuronal replacement from endogenous precursors in the adult brain after stroke. *Nat Med*. 2002;8(9):963–970.